Available online at www.sciencedirect.com
SCIENCE DIRECT
Catalysis Today 111 (2006) 84–93
CATALYSIS TODAY
www.elsevier.com/locate/cattod

# Mechanisms of hydrodesulfurization and hydrodenitrogenation

R. Prins *, M. Egorova, A. Röthlisberger, Y. Zhao, N. Sivasankar, P. Kukula

*Institute for Chemical and Bioengineering, Swiss Federal Institute of Technology (ETH), CH-8093 Zurich, Switzerland*

Available online 14 November 2005

**Abstract**

To study the problems inherent in deep hydrodesulfurization (HDS), the separate and simultaneous HDS of 4,6-dimethyldibenzothiophene and hydrodenitrogenation (HDN) of pyridine were investigated over a Ni-$MoS_2$/γ-$Al_2O_3$ and a Pd/γ-$Al_2O_3$ catalyst. The HDS of 4,6-dimethyldibenzothiophene and its three intermediates, 4,6-dimethyl-tetrahydro-dibenzothiophene, 4,6-dimethyl-hexahydro-dibenzothiophene and 4,6-dimethyl-dodecahydro-dibenzothiophene, demonstrated that, over the Pd catalyst, the (de)hydrogenation reactions were relatively fast compared to the C–S bond breaking reactions, whereas the reverse was true over the metal sulfide catalyst. The methyl groups of 4,6-dimethyldibenzothiophene strongly hinder the direct desulfurization HDS pathway over both catalysts. On the Pd catalyst the hydrogenation pathway is strongly promoted by the methyl groups, so that the total HDS rate does not decrease. Pyridine and piperidine were strong poisons for the hydrogenation pathway and $H_2S$ was a strong poison for the direct desulfurization pathway.

HDN of nitrogen-containing aromatic molecules occurs by hydrogenation of the aromatic heterocycle followed by C–N bond breaking. The C–N bond breaks by substitution of the alkylamine by $H_2S$ to form an alkanethiol, followed by the loss of $H_2S$ by elimination or hydrogenolysis. The $NH_2$-SH substitution does not occur by a classic organic substitution reaction but through a multi-step reaction pathway via an alkylimine. DFT calculations showed that the hydrogenolysis of ethanethiol to ethane and the elimination of ethane are relatively easy reactions.


*Keywords:* Deep hydrodesulfurization; 4,6-Dimethyldibenzothiophene; Hydrodenitrogenation; Mechanism; Substitution; Imine intermediate; Ni-Mo catalyst; Pd catalyst

## 1. Introduction

The maximum amount of sulfur allowed in gasoline and diesel fuel was reduced to 50 ppm in 2005 and will probably be reduced even further by 2010. Deep hydrodesulfurization (HDS) technology must be implemented to attain this low level of sulfur. Nitrogen-containing compounds are harmful in deep HDS, as they inhibit the HDS of sulfur-containing compounds through competitive adsorption [1–5]. This was less of a problem in the past, because the amount of nitrogen-containing molecules in desulfurized naphtha and gas oil was still much smaller than that of the remaining sulfur-containing molecules. At the low sulfur level now required, however, nitrogen-containing compounds compete with the sulfur-containing molecules for the adsorption sites. Therefore, it is important to know how nitrogen-containing molecules influence HDS and how they can be removed by hydrodenitrogenation.

Dibenzothiophene molecules with alkyl groups at the 4 and 6 positions, adjacent to the sulfur atom, are among the molecules that are most difficult to desulfurize and which cause problems in deep HDS [5–7]. Thus, we use 4,6-dimethyldibenzothiophene (4,6-DM-DBT) as a model molecule in our HDS studies. Over metal sulfide as well as over noble metal catalysts the HDS of 4,6-DM-DBT goes through two reaction pathways: direct desulfurization (DDS) by hydrogenolysis of the C–S bonds, which leads to the formation of 3,3′-dimethylbiphenyl, and hydrogenation (HYD) to hydrogenated intermediates, followed by desulfurization to 3,3′-dimethylcyclohexylbenzene and 3,3′-dimethyl-bicyclohexyl. Because the network of the HDS of 4,6-DM-DBT is complex, it does not suffice to study only the reaction of 4,6-DM-DBT. Therefore, we synthesized three intermediates, 4,6-dimethyl-tetrahydro-dibenzothiophene (4,6-DM-TH-DBT), 4,6-dimethyl-hexahydro-dibenzothiophene (4,6-DM-HH-DBT) and 4,6-dimethyl-dodecahydro-dibenzothiophene (4,6-DM-PH-DBT), and studied their HDS. The influence of nitrogen-containing molecules on HDS was studied with the aid of 2-methylpyridine and 2-methylpiperidine. The questions we addressed are: How does

* Corresponding author.
*E-mail address:* roel.prins@chem.ethz.ch (R. Prins).

0920-5861/$ – see front matter © 2005 Elsevier B.V. All rights reserved.
doi:10.1016/j.cattod.2005.10.008

the direct desulfurization reaction (DDS) occur? How does the last part of the hydrogenation route (HYD), the final removal of sulfur from the hydrogenated DBT intermediates, occur?

Hydrodenitrogenation (HDN) has not been studied as intensively as HDS, mainly because in the past it was more important to remove sulfur from fuels than nitrogen. Nelson and Levy proposed that the first step in the HDN of nitrogen-containing aromatic molecules in oil fractions is to transform the strong aromatic C–N bonds into weaker aliphatic C–N bonds by hydrogenation of the heterocyclic aromatic molecules. Thereafter the removal of the nitrogen atom from the resulting alkylamines can take place by nucleophilic substitution and Hofmann β-H elimination [8]. Evidence of both mechanisms has been published [9–12], and it has been suggested that the mechanism depends on the alkylamine and on the catalyst [13]. We found that, over sulfided NiMo, CoMo and Mo on γ-$Al_2O_3$, the substitution mechanism dominates in the HDN of alkylamines with the $NH_2$ group attached to a primary or secondary carbon atom [14–16]. Hofmann β-H elimination hardly occurs in these alkylamines. Nevertheless, a large amount of alkenes is formed in the HDN of alkylamines by fast decomposition of the alkanethiols, formed by the substitution of the alkylamines with $H_2S$. The only amines that react by elimination are the tertiary amines; they react by means of an E1 mechanism [15].

One remaining question is: How does the substitution of the $NH_2$ group by an SH group occur? Does it take place by classic organic substitution chemistry, catalyzed by acidic or metallic (Lewis-acidic) sites, and with inversion of the configuration of the α-carbon atom adjacent to the N atom? Or does the substitution take place by a sequence of reactions, in which dehydrogenated intermediates play an important role? For instance, the sequence dehydrogenation of amine to imine, $H_2S$ addition, ammonia elimination and hydrogenation of the thioaldehyde may transform an alkylamine into an alkanethiol [17]. These questions were answered by using the optically active 2-(*S*)-butylamine as the reactant.

## 2. Experimental

The Ni-$MoS_2$/γ-$Al_2O_3$ catalyst (8 wt.% Mo and 3 wt.% Ni) was prepared by successive incipient wetness impregnation of γ-$Al_2O_3$, drying at 120 °C after each impregnation step and calcining at 500 °C for 4 h [18]. The 0.5 wt.% Pd/$Al_2O_3$ catalyst was prepared by incipient wetness impregnation of γ-$Al_2O_3$ with a 5% aqueous solution of $Pd(NH_3)_4(NO_3)_2$, drying at 120 °C and calcining at 500 °C for 4 h [19].

A sample of 0.05 g catalyst (35–60 mesh) was diluted with 8 g SiC to achieve plug-flow conditions in the continuous-flow fixed-bed reactor. The Ni-$MoS_2$ catalyst was sulfided in situ with a mixture of 10% $H_2S$ in $H_2$ at 400 °C and 1.0 MPa for 4 h. The Pd catalyst was reduced in situ at 300 °C in 0.5 MPa $H_2$ for 2 h. After the activation step (sulfidation or reduction) the pressure was increased to 5.0 MPa and the liquid reactant was fed to the reactor by means of a high-pressure pump. Experiments over the Ni-$MoS_2$ catalyst were carried out at 300–340 °C with a gas feed consisting of 1–6 kPa amine reactant, 1 kPa 4,6-DM-DBT or one of its intermediates, 130 kPa toluene (as solvent), 8 kPa dodecane (reference for GC analysis), 35 kPa $H_2S$ and 4.8 MPa $H_2$. The experiments on the Pd catalyst were performed at 300 °C with a gas feed consisting of 130 kPa decane (solvent), 8 kPa dodecane (for GC analysis), 1 kPa 4,6-DM-DBT or one of its intermediates and 4.9 MPa $H_2$. No $H_2S$ was added to the feed. Piperidine or pyridine was added to the feed to study the influence of nitrogen compounds.

The reaction products of the HDS and HDN reactions were analyzed by off-line gas chromatography with a Varian 3800 GC instrument equipped with a PTA-5 fused silica capillary column (Supelco, 5% diphenylsiloxane/95% dimethylsiloxane, 30 m × 0.25 mm × 0.5 μm). Detection was performed with a flame ionization detector as well as with a pulsed flame photometric detector, which is very useful for detecting small amounts of nitrogen- and sulfur-containing compounds. Weight time was defined as the ratio between the catalyst weight and the molar flow to the reactor. The weight time was changed by varying the flow rates of the liquid and the gaseous reactants, while keeping their ratio constant [18,19].

4,6-DM-TH-DBT was prepared in the same continuous-flow high-pressure unit as used in the HDS and HDN experiments over a 8 wt.% Mo/γ-$Al_2O_3$ catalyst [20] at 320 °C with a gas-phase feed consisting of 130 kPa toluene (as solvent), 2.5 kPa 4,6-DM-DBT (almost the limit of solubility, 45 mg/ml), 20 kPa $H_2S$ and ~4.85 MPa $H_2$. The composition of the product was 69% 4,6-DM-DBT, 18% 4,6-DM-TH-DBT, 6% 4,6-DM-HH-DBT, 1% 4,6-DM-PH-DBT and 6% desulfurized products at a conversion of 31%. After recovering unreacted 4,6-DM-DBT by crystallization in toluene, the remaining mother liquor was evaporated to dryness together with commercial silica. The reaction products were separated by column chromatography over silica, using petroleum ether as the eluent. The fractions containing 4,6-DM-TH-DBT were further purified by vacuum distillation. MS, $^1H$ and $^{13}C$ NMR spectroscopy revealed the final product to be 4,6-dimethyl-1,2,3,4-tetrahydro-dibenzothiophene.

4,6-DM-HH-DBT and 4,6-DM-PH-DBT were prepared by hydrogenation of 4,6-DM-DBT at 200 °C and 15 MPa $H_2$ for 5 h in a 300 ml stainless steel autoclave loaded with 10 g 10 wt.% Pd/C (catalyst), 10 g 4,6-DM-DBT and 180 ml glacial acetic acid. The product consisted of 47% 4,6-DM-DBT, 4% 4,6-DM-TH-DBT, 42% 4,6-DM-HH-DBT, 4% 4,6-DM-PH-DBT and 3% desulfurized products at a conversion of 53%. The catalyst was filtered off and refluxed in chloroform for 1 h to recover the adsorbed product. The filtrates were evaporated to dryness and the unreacted 4,6-DM-DBT was purified by crystallization in toluene. The reaction products were separated twice by column chromatography. Three different isomers of 4,6-DM-HH-DBT were isolated and characterized by $^1H$ and $^{13}C$ NMR spectroscopy, MS/MS experiments and X-ray crystal structure determination: 28% isomer A with the (*4,4a*)-*trans*-(*4a,9b*)-*cis* configuration, 9% isomer B with the (*4,4a*)-*trans*-(*4a,9b*)-*trans* configuration and 63% isomer C with the (*4,4a*)-*cis*-(*4a,9b*)-*cis* configuration. Trace amounts of a fourth diastereomer were observed among the reaction products, but there was too little to isolate for characterization. However, it can have only the (*4,4a*)-*cis*-(*4a,9b*)-*trans* configuration. In

the case of 4,6-DM-PH-DBT, one diastereomer was produced almost exclusively, with the *all-cis* configuration for the six chiral centers of the molecule. For further details see [19].

## 3. Results and discussion

### 3.1. Hydrodesulfurization of 4,6-DM-DBT

#### 3.1.1. Hydrodesulfurization

Scheme 1 represents the product distribution in the HDS of 4,6-DM-DBT over the Ni-$MoS_2$ and Pd catalysts at 300 °C and 5 MPa total pressure. The desulfurized molecules 3,3′-dimethyl-cyclohexylbenzene and 3,3′-dimethyl-bicyclohexyl are the final products of the HYD pathway and 3,3′-dimethyl-biphenyl is the product of the DDS route, because the yields and selectivities of these three products increase continuously as a function of weight time. Over the Ni-$MoS_2$ catalyst only the tetrahydro-intermediate 4,6-DM-TH-DBT was observed (Fig. 1) [21], suggesting that the subsequent hydrogenation to the hexahydro-intermediate 4,6-DM-HH-DBT is rate determining. Over the Pd catalyst, on the other hand, significant amounts of all three hydrogenated intermediates, 4,6-DM-TH-DBT, 4,6-DM-HH-DBT and 4,6-DM-PH-DBT, were detected (Fig. 2) [19]. Apparently, on Pd the hydrogenation reactions are relatively fast and the C–S bond breaking reactions are slow. 4,6-DM-TH-DBT, 4,6-DM-HH-DBT and 4,6-DM-PH-DBT form quickly and act as reaction intermediates with their yields passing through a maximum (Fig. 2). 4,6-DM-TH-DBT is the primary product of the HYD pathway and 4,6-DM-TH-DBT and 4,6-DM-HH-DBT form in a constant ratio. This suggests that they are in equilibrium and that the transformation of 4,6-DM-TH-DBT to 4,6-DM-HH-DBT is relatively rapid.

Experiments starting with the intermediates of 4,6-DM-DBT confirmed the different behaviour of the Ni-$MoS_2$ and Pd catalysts. Over Ni-$MoS_2$, the reactions went forward but not backward, whereas over Pd the reactions occurred in both directions. Thus, in the reaction of 4,6-DM-TH-DBT over Ni-$MoS_2$, 4,6-DM-HH-DBT and 4,6-DM-PH-DBT, as well as the final products 3,3′-dimethyl-cyclohexylbenzene and 3,3′-dimethyl-bicyclohexyl, were produced at 300 and 320 °C (Fig. 3). Over Pd, 4,6-DM-DBT was also produced (Fig. 4).

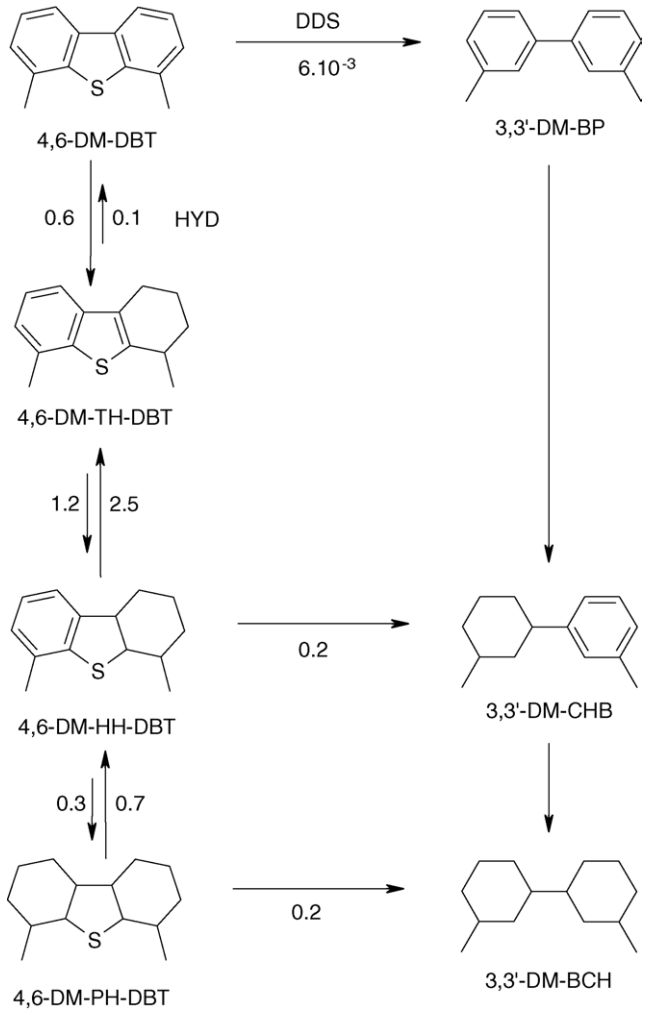


Scheme 1. Reaction network of the HDS of 4,6-DM-DBT. The pseudo first-order rate constants (in mol/(g min)) were obtained over 0.5 wt.% Pd/γ-$Al_2O3$ at 300 °C and 5 MPa.

Similarly, 4,6-DM-PH-DBT, 3,3′-dimethyl-cyclohexylbenzene and 3,3′-dimethyl-bicyclohexyl were produced in the reaction of 4,6-DM-HH-DBT over Ni-$MoS_2$, while over Pd 4,6-DM-TH-DBT and even 4,6-DM-DBT were also produced. Hydrogenation and dehydrogenation reactions apparently occur

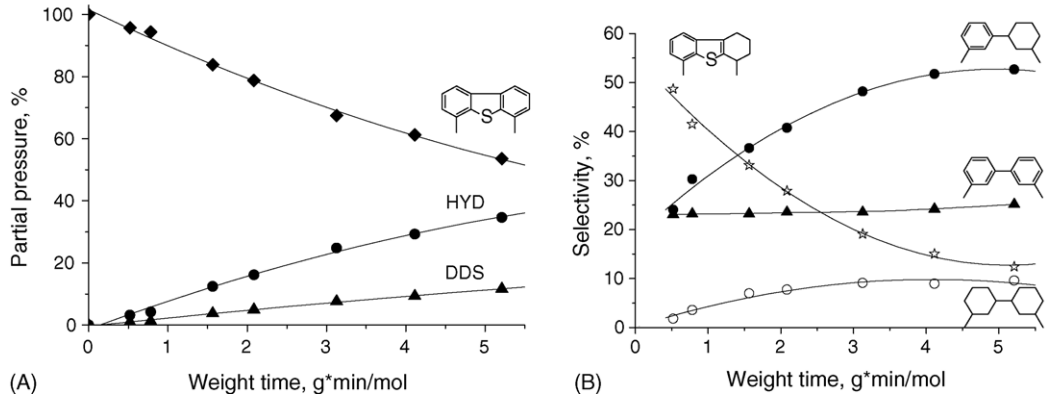


Fig. 1. Relative partial pressures (A) and selectivities (B) in the HDS of 4,6-DM-DBT over NiMo/γ-$Al_2O_3$ at 340 °C (◆, 4,6-DM-DBT; ▲, 3,3′-DM-BP; ☆, 4,6-DM-TH-DBT; ●, 3,3′-DM-CHB; ○, 3,3′-DM-BCH).

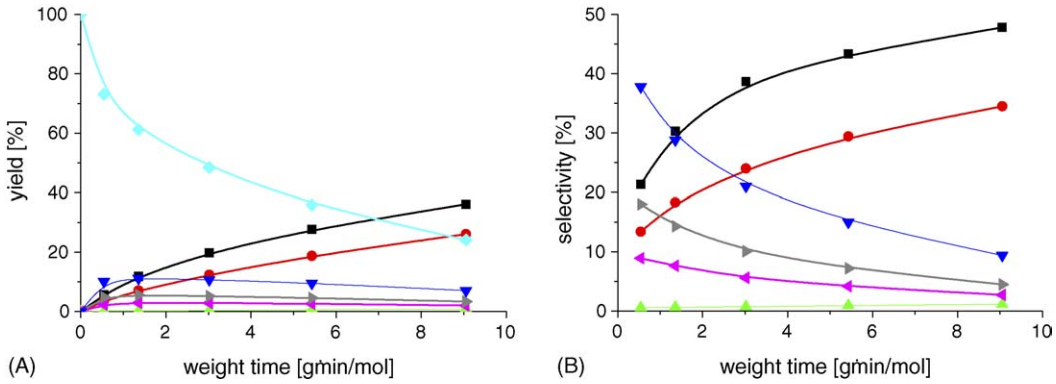


Fig. 2. Product yields (A) and selectivities (B) in the HDS of 4,6-DM-DBT over Pd/γ-$Al_2O_3$ at 300 °C (◆, 4,6-DM-DBT; ▲, 3,3′-DM-BP; ▼, 4,6-DM-TH-DBT; ▶, 4,6-DM-HH-DBT; ◀, 4,6-DM-PH-DBT; ●, 3,3′-DM-CHB; ■, 3,3′-DM-BCH).

easily on the Pd surface and all the sulfur-containing intermediates are always present, even 4,6-DM-DBT.

Pseudo first-order rate constants were determined from the disappearance of the reactants at small weight time and the resulting values for the Pd/γ-$Al_2O_3$ catalyst are presented in Scheme 1. The rate constants for the direct sulfur removal show that 4,6-DM-DBT is extremely difficult to desulfurize, whereas 4,6-DM-HH-DBT and 4,6-DM-PH-DBT have much larger rate constants for sulfur removal. In the flat 4,6-DM-DBT molecule the methyl groups and the sulfur atom are in the plane of the molecule. The methyl groups adjacent to the sulfur atom are more spacious than the σ orbitals on the sulfur atom and hinder the molecule from binding to the catalyst surface via the sulfur atom, perpendicular to the catalyst surface. Therefore, the adsorption of 4,6-DM-DBT in the σ mode is much weaker than that of DBT and the DDS pathway is strongly suppressed. Hydrogenation of 4,6-DM-DBT takes place via π adsorption, with the molecule flat on the catalyst surface. In this adsorption

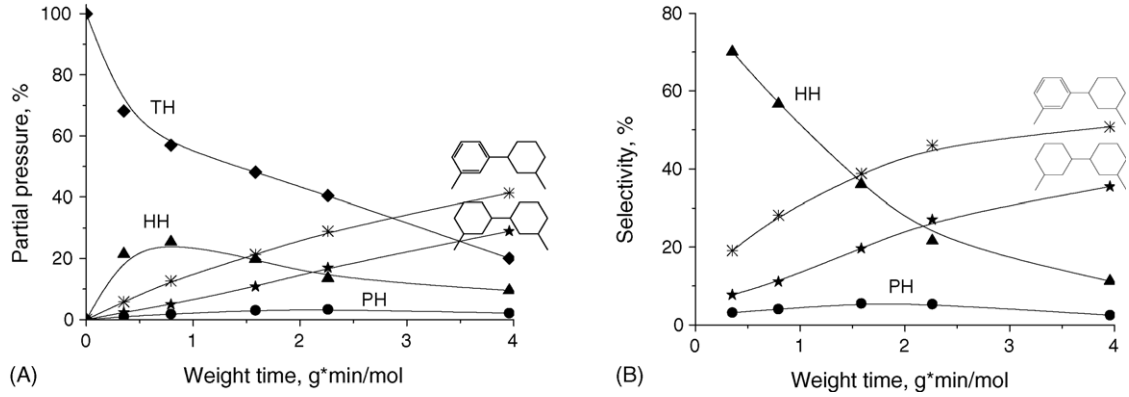


Fig. 3. Relative partial pressures (A) and selectivities (B) in the HDS of 4,6-DM-TH-DBT over NiMo/γ-$Al_2O_3$ at 320 °C as a function of weight time (◆, 4,6-DM-TH-DBT; ▲, 4,6-DM-HH-DBT; ●, 4,6-DM-PH-DBT; *, 3,3′-DM-CHB; ★, 3,3′-DM-BCH).

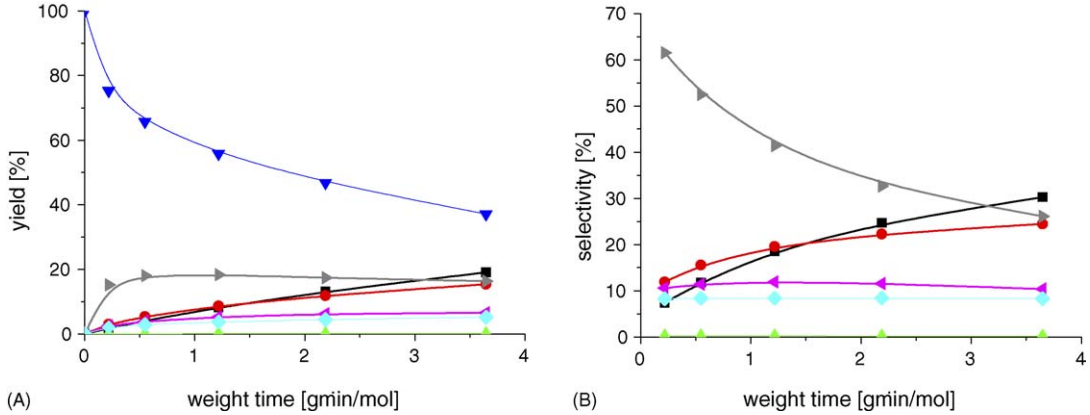


Fig. 4. Product yields (A) and selectivities (B) in the HDS of 4,6-DM-TH-DBT over Pd/γ-$Al_2O_3$ at 300 °C (◆, 4,6-DM-DBT; ▲, 3,3′-DM-BP; ▼, 4,6-DM-TH-DBT; ▶, 4,6-DM-HH-DBT; ◀, 4,6-DM-PH-DBT; ●, 3,3′-DM-CHB; ■, 3,3′-DM-BCH).

mode the methyl groups do not hinder the adsorption. Because of their electron-donating influence they even make the HYD pathway in the HDS of 4,6-DM-DBT faster than that of DBT. As a consequence of these effects of the methyl groups, the DDS rate constant of the Ni-$MoS_2$ catalyst (measured at low conversion) decreases from 2.05 for DBT to 0.08 mol/(g min) for 4,6-DM-DBT, when there is no $H_2S$ in the feed, while the hydrogenation rate constant decreases from 0.28 to 0.12 mol/(g min) [20]. This is a decrease of more than an order of magnitude in the total rate constant. For Pd the DDS rate constant decreases even more strongly, from 0.34 to 0.01 mol/(g min). At the same time, however, the hydrogenation pathway, which requires π adsorption, is promoted from 0.11 to 0.57 mol/(g min), so that the total rate constant over Pd even increases from 0.45 to 0.58 mol/(g min) [19].

The strong suppression of the DDS pathway by the methyl groups explains why 4,6-DM-DBT mainly reacts via the HYD pathway over both catalysts. Since the hydrogenation pathway is strongly promoted by the methyl groups over the Pd catalyst, the Pd catalyst has a higher conversion than the Ni-$MoS_2$ catalyst in the HDS of 4,6-DM-DBT. Nevertheless, over the Pd catalyst there is a substantial yield of the sulfur-containing intermediates, while over the Ni-$MoS_2$ catalyst their yield is much lower. This is due to the fact that, also in the hydrogenation pathway, the C–S bond can be broken only when the molecule is bonded to the catalyst in the σ mode. Either this C–S bond breaking is very difficult over Pd, or few exposed sites are present on the Pd surface, to which the sulfur atom of 4,6-DM-HH-DBT and 4,6-DM-PH-DBT can bind.

Hydrogenation of 4,6-DM-DBT leads to a flexible cyclohexyl ring. The hydrogenated ring can adopt several conformations, in some of which the bulky methyl substituent is rotated away from the sulfur atom. This decreases the steric hindrance of the methyl groups located at positions 4 and 6 and makes the sulfur atom more accessible for desulfurization [22]. Furthermore, as molecular modeling calculations showed, the lengths of the C–S bonds increase with the degree of saturation of the molecules, making these bonds more reactive. Hydrogenation of 4,6-DM-DBT to 4,6-DM-TH-DBT is not sufficient, however. The fact that many more sulfur-containing intermediates are observed in the HDS of 4,6-DM-DBT than in that of DBT means that the removal of sulfur from 4,6-DM-TH-DBT is much slower than from TH-DBT [20]. Although the hydrogenated ring of 4,6-DM-TH-DBT is not flat, the double bond diminishes its mobility and the methyl group of the hydrogenated ring can hardly rotate away from the plane of the molecule, and thus from the sulfur atom. Thus, adsorption of 4,6-DM-TH-DBT in the σ mode is still strongly hindered and direct C–S bond breaking in 4,6-DM-TH-DBT is almost as difficult as in 4,6-DM-DBT. 4,6-DM-HH-DBT and 4,6-DM-PH-DBT, on the other hand, are more flexible and one methyl group of 4,6-DM-HH-DBT and both of 4,6-DM-PH-DBT can rotate away from the sulfur atom. This enables a stronger σ adsorption and reasonably high rate constants for the C–S bond cleavage of 4,6-DM-TH-DBT to 3,3′-dimethyl-cyclohexylbenzene and of 4,6-DM-PH-DBT to 3,3′-dimethyl-bicyclohexyl.

### 3.1.2. *Influence of N-compounds and $H_2S$*

2-Methylpyridine and 2-methylpiperidine strongly inhibit the conversion of 4,6-DM-DBT over the Ni-$MoS_2$ catalyst at 340 °C [20,21]. With 2 kPa amine in the feed the conversion of 1 kPa 4,6-DM-DBT decreased by a factor 5 and the HYD pathway was more strongly suppressed than the DDS pathway. At high amine concentration (6 kPa) the conversion of 4,6-DM-DBT was further reduced and the only products were 3,3′-dimethylbiphenyl (DDS pathway) and 4,6-DM-TH-DBT (HYD pathway). As long as the HDN of the amine did not proceed sufficiently, 4,6-DM-TH-DBT did not react further. The amine appears to adsorb more strongly on the catalytically active site than 4,6-DM-TH-DBT. The HDS of the intermediates of 4,6-DM-DBT did indeed show that the HDS reaction was strongly inhibited by nitrogen-containing compounds. For instance, the presence of 0.1 kPa 2-methylpiperidine suppressed the conversion of 1 kPa 4,6-DM-HH-DBT below 2% at 300 °C.

Similar inhibition effects of the amine were observed over the Pd catalyst at 300 °C [19]. Piperidine and pyridine strongly inhibited both HDS pathways in the HDS of 4,6-DM-DBT and showed a similar influence. In the presence of 0.5 kPa amine the conversion of 4,6-DM-DBT decreased by a factor of four and the HYD pathway was more strongly inhibited than the DDS pathway. Although the hydrogenation activity of the catalyst was diminished by the presence of the amine, the hydrogenation was still appreciable and all three intermediates (tetra, hexa and dodecahydro) were observed. The Pd catalyst clearly functions better than the Ni-$MoS_2$ catalyst in the presence of amines.

$H_2S$ inhibits the HDS of all sulfur-containing molecules [5]. It inhibits the DDS as well as the HYD pathway of DBT and 4,6-DM-DBT, but it inhibits the DDS pathway to a greater extent [20,23]. In this respect, $H_2S$ has the opposite effect of the amines. In the absence of $H_2S$, the Ni-$MoS_2$ catalyst reacts about seven times faster via the DDS than via the HYD pathway in the HDS of DBT. In the presence of 100 kPa $H_2S$, however, the DDS pathway was only twice as fast. The inhibition of $H_2S$ is weaker for 4,6-DM-DBT than for DBT because of the large HYD contribution to the HDS of 4,6-DM-DBT and the smaller inhibitory effect of $H_2S$ on the HYD pathway. Although the HYD pathway of the HDS of 4,6-DM-DBT was not as strongly suppressed by $H_2S$, the fraction of the partially hydrogenated intermediates in the HYD pathway increased at increasing $H_2S$ partial pressure. This shows again that DDS activity is required for the final C–S bond breaking.

The different influence of amines and $H_2S$ on the DDS and HYD pathways suggests that both HDS pathways are determined by the conformation of the adsorbed DBT and 4,6-DM-DBT molecules. In agreement with other authors [24,25], we believe that DDS occurs through σ adsorption via the sulfur atom and HYD through π adsorption of the reactant via the aromatic system. As will be explained in the next section, it is unnecessary to assume a common intermediate for the DDS and HYD pathways, as some have done [7].

It is generally assumed that the catalytically active sites in Mo/γ-$Al_2O_3$ hydrotreating catalysts are the molybdenum atoms at the edges and corners of the $MoS_2$ crystallites, which have at

least one sulfur vacancy. This vacancy enables chemical adsorption of the reacting molecule on the molybdenum atom [26–28]. The addition of nickel substantially increases the HDS and HDN activities of a $MoS_2/\gamma$-$Al_2O_3$ catalyst. Density functional theory (DFT) calculations show that the most stable position for the Ni promoter is at the edge; there it substitutes the molybdenum atom [29] and forms the so-called Ni–Mo–S phase [27]. DFT calculations suggest that the combined action of the promoter and the molybdenum atom is responsible for the catalysis [29–31]. It was shown that a sulfur atom between a nickel and a molybdenum atom is less strongly bonded than a sulfur atom between two molybdenum atoms and can be removed more easily, thus creating a vacancy. Therefore, the promoter may enhance the intrinsic rate of the C–S bond cleavage by increasing the electron density on the active Mo sites as well as by creating a larger number of sulfur vacancies on the Ni-promoted catalysts.

We suggest that the DDS sites, on which the C–S bonds of DBT and 4,6-DM-DBT are broken, and the sites on which sulfur is removed from the partially hydrogenated intermediates are the same and constitute a sulfur vacancy on the catalyst surface. That would explain why $H_2S$ strongly inhibits the sulfur removal in both pathways. The hydrogenation of DBT and 4,6-DM-DBT, on the other hand, is much less affected by $H_2S$. This suggests that vacancies are not required for the flat π adsorption of the sulfur-containing molecules and that hydrogenation may even occur over a surface that is completely covered by sulfur. Another possibility is that the DDS sites are located at the edges of the $MoS_2$ slabs and that the HYD sites are located at the corners, which are less sensitive to the presence of $H_2S$ and allow the π adsorption of the spacious molecules. Because of the low symmetry of corner sites, DFT calculations with large unit cells must be performed in the future.

### 3.1.3. C–S bond breaking

The breaking of the C–S bond may, in principle, take place by elimination to form $H_2S$ and an alkene or by hydrogenolysis to form $H_2S$ and an alkane. In the latter reaction C–S bonds are broken and C–H and S-H bonds formed simultaneously. For aliphatic thiols both reactions are known to occur. Thus, methanethiol easily reacts to methane [32] and ethanethiol to ethane and ethene over metal sulfide catalysts [33]. To investigate the mechanism of C–S bond breaking, DFT calculations of the adsorption of alkanethiols, C–S bond breaking and the formation and desorption of alkene and alkane at different sulfur and hydrogen coverages of the catalytically active (1 0 0) surface of 2H-$MoS_2$ were performed [34]. We chose the simplest alkanethiol, $CH_3SH$, because only hydrogenolysis to $CH_4$ can take place, and the next simplest alkanethiol, $C_2H_5SH$, because this molecule allows elimination to be studied as well. Using density functional theory (DFT), we calculated the minimum energy path for the alkanethiol dissociation and determined the order of the chemical reaction steps, the various energies of the reactions and the activation barriers. $CH_3SH$ and $C_2H_5SH$ first adsorb molecularly with their S atom in a bridging mode between two surface Mo atoms followed by S–H bond cleavage with moderate activation energy. The subsequent concerted C–S bond breaking and alkane formation occur by reaction of the adsorbed $CH_3S$ or $C_2H_5S$ group with the H atom of a neighbouring SH group at the molybdenum sulfide surface. Sulfur atoms, hydrogen atoms adsorbed on sulfur atoms and promoter atoms (Co and Ni) at the catalyst surface weaken the bonding of adsorbed $CH_3S$ and $C_2H_5S$ and lower the energy barrier for alkane formation. The C–S bond breaking, resulting in methane and ethane formation, proceeds with a similar energy barrier. This shows that the product depends on the reaction conditions. Alkenes are the main product at atmospheric pressure, while at elevated pressure (1–5 MPa) alkenes and alkanes are produced in comparable amounts over metal sulfide catalysts.

Not only alkanethiols but also arylthiols undergo a reaction that appears to be a direct C–S bond breaking. For instance, thiophenol reacts mainly to benzene [35] and, as discussed above, dibenzothiophene to biphenyl. The mechanism of the direct desulfurization in arylthiols may consist of an actual hydrogenolysis reaction. In this case, thiophenol and hydrogen atoms on the catalyst surface react directly to benzene and dibenzothiophene and hydrogen atoms react directly to biphenyl. Other authors believe that the mechanism consists of hydrogenation of thiophenol or dibenzothiophene to dihydrothiophenol or dihydrodibenzothiophene, followed by elimination of $H_2S$ to give benzene or biphenyl, respectively [7]. Future theoretical calculations may show whether dihydrodibenzothiophene is an intermediate, the energy of which is too high, and whether hydrogenolysis is more likely, as suggested by organometallic studies of the desulfurization of thiols. Thus, Curtis and Druker showed that the association of aliphatic as well as aromatic thiols with a $Cp'_2Mo_2Co_2S_3(CO)_4$ cluster occurs by rearrangement of the cluster and that the coordination of the thiol to the cluster results in substantial weakening of its C–S bond [36]. They suggested that this association is the rate-determining step in the desulfurization reaction and that the subsequent cleavage of the C–S bond occurs rapidly.

How the tetrahydro-, hexahydro- and perhydro-intermediates in the HDS of 4,6-DM-DBT are desulfurized, by elimination or hydrogenolysis, is unknown. $H_2S$ elimination from 4,6-dimethyl-1,2,3,4-tetrahydro-dibenzothiophene is impossible; thus, 4,6-DM-TH-DBT can only react by hydrogenolysis. As discussed in Section 3.1.1, the methyl group in the partially hydrogenated ring of 4,6-DM-TH-DBT can barely rotate and, thus, hydrogenolysis is probably as difficult as in 4,6-DM-DBT. The more common trans elimination, with the H atom on the β-carbon atom in the *trans* position to the S atom on the α-carbon atom, is impossible for 4,6-DM-HH-DBT and 4,6-DM-PH-DBT. *Cis* elimination is possible for the most abundant hexahydro intermediates A and C. Nevertheless, we did not find any olefins among the final products of the HDS of 4,6-DM-HH-DBT. This suggests that hydrogenolysis is responsible for the breaking of both its C–S bonds. Only in the HDS of 4,6-DM-PH-DBT over Ni-$MoS_2$ did we observe a product with a mass number two units lower than that of 3,3′-dimethylbicyclohexyl. This suggests that the first C–S bond of 4,6-DM-PH-DBT is broken by hydrogenolysis and that the

second is (partially) broken by elimination from 3,3′-dimethylbicyclohexyl-2-thiol.

### 3.2. Hydrodenitrogenation

Nelson and Levy already indicated in 1979 that, in contrast to HDS, the direct breakage of the C–N bond is impossible in heterocyclic aromatic molecules [8]. It is even difficult in exocyclic molecules such as aniline, for which hydrogenation to cyclohexylamine precedes C–N bond breaking [17]. This leaves hydrogenation as the dominant pathway in HDN. Once the aromaticity is lost and aliphatic C–N bonds have formed, C–N bond breaking becomes possible. Because of an abundance of alkenes in the HDN product, elimination of ammonia to form alkenes was, for a long time, considered to be the mechanism responsible for C–N bond breaking [9–13]. Only when a β-hydrogen atom is not available, as in benzylamine, was nucleophilic substitution presumed to play a role [10]. However, as we have already published [14–16] and as will be summarized in the next section, this is untrue. Only for alkylamines with the nitrogen atom linked to a tertiary carbon atom does elimination dominate. In all other cases the dominant mechanism is nucleophilic substitution by $H_2S$.

#### 3.2.1. Substitution rather than elimination

In the simultaneous HDN of pentylamine and the HDS of hexanethiol at 320 °C and 3 MPa the HDN products over the Ni-$MoS_2$ catalyst were pentanethiol, dipentylamine, pentene and pentane. By determining the product selectivities at short contact time we were able to distinguish between primary and secondary products [14,16]. The selectivities of dipentylamine and pentanethiol extrapolated to non-zero values with decreasing weight time, indicating that they were primary products. The pentene and pentane selectivities extrapolated to a non-zero value with decreasing weight time, but at the same time the selectivities initially increased with weight time. The non-zero selectivities at time zero suggest that these products are primary, while the increase in selectivity indicates that they are secondary (or even tertiary) products. The fact that the pentenes and pentane behave as primary as well as secondary products is caused by the complexity of the HDN reaction network. Pentene and pentane form by decomposition of pentanethiol, which forms from pentylamine in a direct step or indirectly in several steps, as we will show below. Thus, pentene and pentane are actually secondary or tertiary products of the alkylamine.

The alkene/alkane ratio was used to confirm that the alkenes are produced via the alkanethiol [14,16]. If an alkylamine reacts to an intermediate alkanethiol and subsequently to alkene and alkane, then the alkene/alkane ratio is determined by the thiol and should be the same as in the HDS of the alkanethiol. Since the branching ratio is sensitive to the presence and the partial pressures of alkylamine and alkanethiol, this ratio was always determined in a simultaneous HDS and HDN experiment, in which pentylamine and hexanethiol were both present. The hexene/hexane ratio, obtained in the HDS of hexanethiol, was similar to the pentene/pentane ratio obtained in the HDN of pentylamine. This demonstrates that alkenes do not form by elimination from the alkylamine.

Pentanethiol was a primary product in the HDN of pentylamine over $NiMo/Al_2O_3$, as shown by the non-zero selectivity at time zero (Fig. 5). Pentanethiol can actually form in two ways, by substitution of pentylamine with $H_2S$:

$$C_5H_{11}NH_2 + H_2S \rightarrow C_5H_{11}SH + NH_3 \quad (1)$$

and by substitution of dipentylamine with $H_2S$:

$$C_5H_{11}NH_2 + C_5H_{11}NH_2 \rightarrow C_5H_{11}NHC_5H_{11} + NH_3 \quad (2)$$

$$C_5H_{11}NHC_5H_{11} + H_2S \rightarrow C_5H_{11}SH + C_5H_{11}NH_2 \quad (3)$$

Pentanethiol is a primary product in Eq. (1) and a secondary product in Eq. (3). Eq. (1) explains why the selectivity of pentanethiol is not zero at $\tau = 0$. For sulfided $Mo/Al_2O_3$ at 100 kPa $H_2S$, the selectivity–weight time curve of pentanethiol even showed a maximum. The initial increase in the pentanethiol selectivity with increasing weight time proves that dipentylamine, formed by the disproportionation of pentylamine (Eq. (2)), reacts fast with $H_2S$ to form pentanethiol and

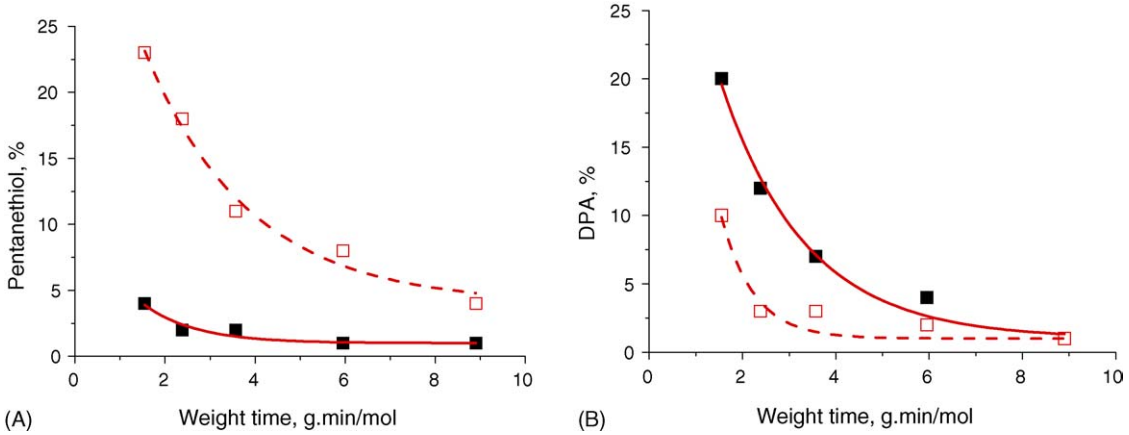


Fig. 5. Product selectivities of pentanethiol (A) and dipentylamine (B) in the HDN of pentylamine in the presence of hexanethiol at 10 kPa (■) and 100 kPa (□) $H_2S$, and 320 °C over sulfided $NiMo/Al_2O_3$ (DPA = dipentylamine).

pentylamine (Eq. (3)). The decrease at higher weight time is because of the reaction of the thiol to an alkene by elimination and to an alkane by hydrogenolysis. The primary as well as the secondary formation of pentanethiol is directly related to the primary as well as the secondary formation of pentene and pentane, because they are the products of the decomposition of pentanethiol.

### 3.2.2. Substitution mechanism

To determine how the substitution of the amine group of an alkylamine by a sulfhydryl group takes place we used 2-(*S*)-butylamine as the substrate [37]. Over sulfided NiMo/γ-$Al_2O_3$, the conversion was 28% at 300 °C and 29% butane, 1-butene, *cis*-2-butene and *trans*-2-butene, 33% 2-butanethiol and 38% di-*sec*-butylamine were produced. The thiol and unreacted amine were derivatized with the chiral Moscher's acid chloride. The chromatogram of the resulting diastereomers of 2-butanethiol showed that the 2-butanethiol formed in the reaction of 2-(*S*)-butylamine was racemic. The optical purity of the 2-(*S*)-butylamine had decreased during the HDN reaction; we observed 60% racemization under our reaction conditions. The isomers of di-2-butylamine were not derivatized but were analyzed directly by chiral gas chromatography. With 2-(*S*)-butylamine we obtained 20% (*R*,*R*)-, 32% (*S*,*S*)- and 48% (*R*,*S*)-di-*sec*-butylamine.

The same amounts of 2-(*S*)- and 2-(*R*)-butanethiol, formed from pure 2-(*S*)-butylamine, show that the formation of the alkanethiol from the alkylamine does not proceed stereoselectively but proceeds with a loss of chirality of the α-carbon atom. The extent of racemization of the unreacted 2-butylamine was, however, lower (60%) than that of the 2-butanethiol product (100%). This indicates that the racemization of the thiol took place during the substitution reaction. The racemization can be explained by an amine-to-thiol reaction by dehydrogenation of 2-butylamine to 2-butylimine, followed by the addition of $H_2S$ to give a thio-hemiaminal (Scheme 2). Elimination of ammonia from this intermediate and hydrogenation of the resulting thioketone gives 2-butanethiol. The α-carbon atom is involved twice in a double bond and, thus, complete scrambling of the original chirality takes place at this carbon atom. The first racemization occurs during the dehydrogenation of 2-butylamine to 2-butylimine. We did not observe 2-butylimine in our reaction products, since it is a very reactive intermediate. However, the equilibrium between 2-butylamine and 2-butylimine shifts toward the imine at high reaction temperature, and the racemization of 2-butylamine can only be explained by imine formation.

The formation of di-*sec*-butylamine cannot proceed by a classic organic disproportionation reaction, in which a 2-(*S*)-butylamine molecule reacts with another 2-(*S*)-butylamine molecule to di-2-butylamine and ammonia, because in that case the only product would be (*R*,*S*)-di-*sec*-butylamine, the mesoform. If some 2-(*R*)-butylamine forms by isomerization, then 2-(*S*)-butylamine and 2-(*R*)-butylamine should produce equal amounts of the (*S*,*S*) and (*R*,*R*) isomers, which was not the case. Imine intermediates can also explain the observed stereoisomers of di-*sec*-butylamine. Dehydrogenation of 2-(*S*)-butylamine to 2-butylimine, followed by the addition of a molecule of 2-(*S*)-butylamine, elimination of ammonia and hydrogenation of the resulting di-*sec*-butylimine would give an equimolar mixture of (*S*,*S*)- and (*R*,*S*)-di-*sec*-butylamine (Scheme 2). In all cases, also when racemization of 2-(*S*)-butylamine takes place, half of the di-*sec*-butylamine product is (*R*,*S*)-di-*sec*-butylamine. This is exactly what we observed. The larger amount of (*S*,*S*)-di-*sec*-butylamine than of (*R*,*R*)-di-*sec*-butylamine is due to the fact that, at the beginning of the reaction, only 2-(*S*)-butylamine is present, while later 2-(*R*)-butylamine forms by racemization of 2-(*S*)-butylamine. The racemization of 2-(*S*)-butylamine to 2-(*R*)-butylamine and back can occur via the same 2-butylimine intermediate, as proposed for the formation of the 2-butanethiol and di-*sec*-butylamine.

The HDN products and their configurations, as well as the racemization of the alkylamine reactant, can thus be explained by a mechanism, in which imines act as intermediates. Imines were observed in the HDN of alkylamines over metal sulfide catalysts [14]. The formation of imines would be in accordance with recent studies, which demonstrate that the edges of $MoS_2$ and Co and Ni-promoted $MoS_2$ have metallic properties. DFT calculations indicated that the edges of $MoS_2$ have metallic properties [29,30,38] and STM studies of $MoS_2$ crystallites on a gold support confirmed a high electron density on the metal and sulfur atoms at the edges [39].

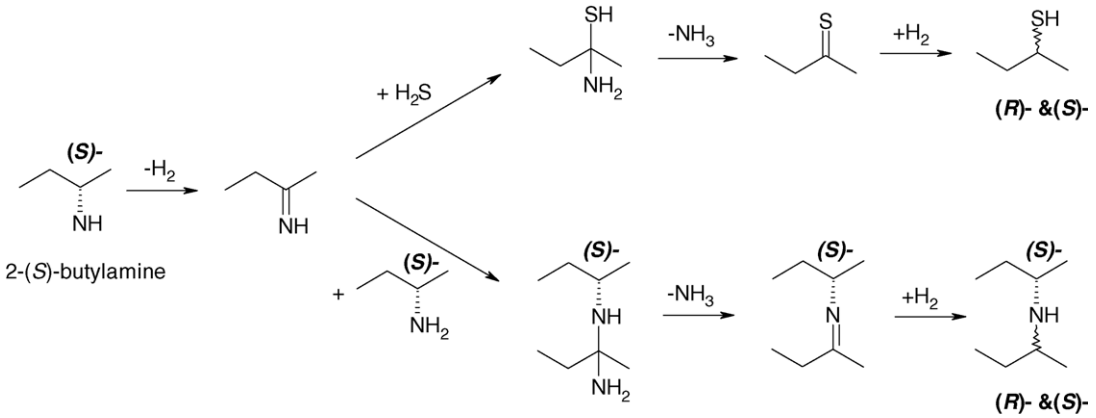


Scheme 2. Substitution of 2-(*S*)-butylamine by $H_2S$ to 2-(*R*)- and 2-(*S*)-butanethiol and by another amine molecule to a di-*sec*-butylamine by means of an imine intermediate.

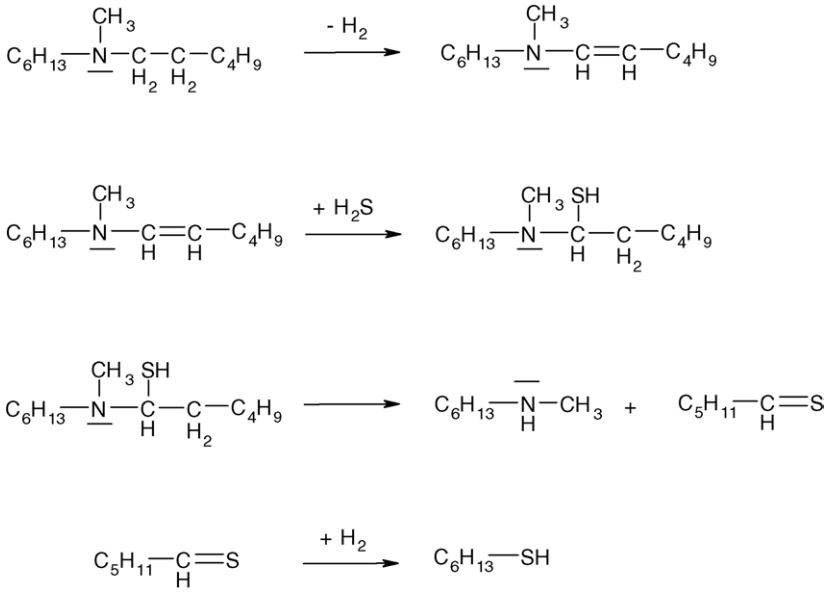

Scheme 3. Mechanism of the substitution of *N*,*N*-dihexylmethylamine by $H_2S$ to *N*-hexylmethylamine and hexanethiol by means of an enamine intermediate.

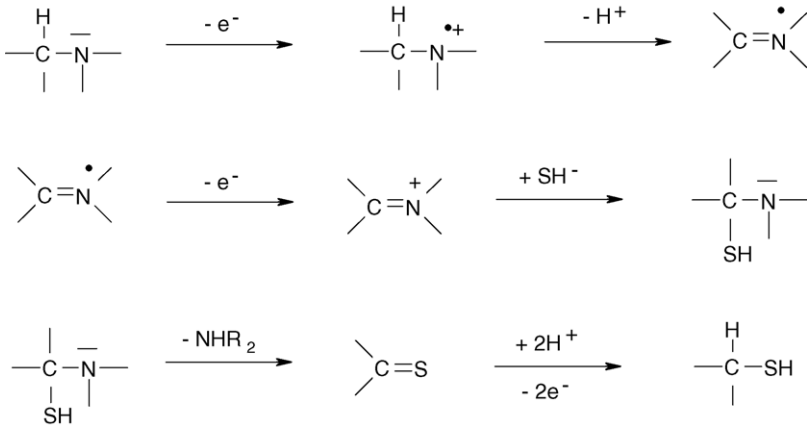

Scheme 4. Mechanism of the substitution of an alkylamine with $H_2S$ to an alkanethiol by means of an imine cation intermediate.

Trialkylamines cannot form imines but can form the related enamines by β-H elimination (Scheme 3). If a β-H atom is not available, then the corresponding alkyl group cannot be replaced by $H_2S$ in the substitution reaction. In that case, *N*-methyldihexylamine can react to *N*-methylhexylamine but not to dihexylamine. However, the experiment showed that almost the same amounts of *N*-methylhexylamine and dihexylamine formed [37]. This cannot be explained by enamine intermediates. The closely related iminium ion intermediate can, however, explain all the observations. Instead of assuming that the reactions take place by dehydrogenation of the alkylamine, one can assume that the reactions occur by the removal of electrons and protons. Alkylamines are known to react to iminium cations by a double oxidation and proton abstraction (Scheme 4). The methyl group of tertiary amines that carry a methyl group, like *N*,*N*-dimethylhexylamine and *N*-methyldihexylamine, cannot react to an imine but can react to a *N*,*N*-dialkylmethyliminium cation. This explains why the methyl group of these tertiary amines can also react. At the same time, it indicates that the surface of the metal sulfides does not act as a metal but rather as a redox-proton system. The metal cations function as catalytic reduction–oxidation centers and the hydrogen atoms on the sulfur atoms as protons.

## 4. Conclusions

The results of the HDS of 4,6-DM-DBT and its three intermediates, 4,6-DM-TH-DBT, 4,6-DM-HH-DBT and 4,6-DM-PH-DBT demonstrated that the same reaction network applies for the sulfidic Ni-$MoS_2$ catalysts and for the metallic Pd catalyst. The direct desulfurization pathway is of minor importance; most 4,6-DM-DBT molecules react through the hydrogenation pathway. In this pathway, the reaction occurs by a sequence of hydrogenation steps of 4,6-DM-DBT to

4,6-DM-TH-DBT and on to 4,6-DM-HH-DBT and 4,6-DM-PH-DBT. Desulfurization takes place by C–S bond breaking of the latter two intermediates. Desulfurization from these two molecules is orders of magnitude faster than that from DMDBT, because the methyl group in the hydrogenated ring can be rotated away from the sulfur atom and because the C–S bond is weaker after hydrogenation. Over the Pd catalyst, the (de)hydrogenation reactions are relatively fast and the desulfurization reactions are rate limiting. Over the $NiMoS_2$ catalyst all the reactions are the same order of magnitude.

## References


[1] C.N. Satterfield, M. Modell, J.A. Wilkens, Ind. Eng. Chem. Process. Des. Dev. 19 (1980) 154.
[2] M. Nagai, T. Kabe, J. Catal. 81 (1983) 440.
[3] T. Koltai, M. Macaud, A. Guevara, E. Schulz, M. Lemaire, R. Bacaud, M. Vrinat, Appl. Catal. A 231 (2002) 253.
[4] C. Kwak, J.J. Lee, J.S. Bae, S.H. Moon, Appl. Catal. B 35 (2001) 59.
[5] M.J. Girgis, B.C. Gates, Ind. Eng. Chem. Res. 30 (1991) 2021.
[6] D.D. Whitehurst, T. Isoda, I. Mochida, Adv. Catal. 42 (1998) 345.
[7] F. Bataile, J.L. Lemberton, P. Michaud, G. Pérot, M. Vrinat, M. Lemaire, E. Schulz, M. Breysse, S. Kasztelan, J. Catal. 191 (2000) 409.
[8] N. Nelson, R.B. Levy, J. Catal. 58 (1979) 485.
[9] J.L. Portefaix, M. Cattenot, M. Guerriche, J. Thivolle-Cazat, M. Breysse, Catal. Today 10 (1991) 473.
[10] L. Vivier, V. Dominguez, G. Perot, S. Kasztelan, J. Mol. Catal. 67 (1991) 267.
[11] J.L. Portefaix, M. Cattenot, M. Guerriche, M. Breysse, Catal. Lett. 9 (1991) 127.
[12] M. Breysse, J. Afonso, M. Lacroix, J.L. Portefaix, M. Vrinat, Bull. Soc. Chim. Belg. 100 (1991) 923.
[13] M. Cattenot, J.L. Portefaix, J. Afonso, M. Breysse, M. Lacroix, G. Perot, J. Catal. 173 (1998) 366.
[14] Y. Zhao, P. Kukula, R. Prins, J. Catal. 221 (2004) 441.
[15] Y. Zhao, R. Prins, J. Catal. 222 (2004) 532.
[16] Y. Zhao, R. Prins, J. Catal. 229 (2005) 213.
[17] R. Prins, Adv. Catal. 46 (2001) 399.
[18] M. Egorova, Y. Zhao, P. Kulula, R. Prins, J. Catal. 206 (2002) 263.
[19] A. Röthlisberger, R. Prins, J. Catal. 235 (2005) 229.
[20] M. Egorova, R. Prins, J. Catal. 225 (2004) 417.
[21] M. Egorova, R. Prins, J. Catal. 224 (2004) 278.
[22] T. Kabe, A. Ishihara, Q. Zhang, Appl. Catal. A 97 (1993) L1.
[23] Q. Zhang, W. Qian, A. Ishihara, T. Kabe, Sekiyu Gakkaishi 40 (1997) 185.
[24] C.N. Satterfield, M. Modell, J.F. Mayer, AIChE J. 21 (1975) 1100.
[25] S. Harris, R.R. Chianelli, J. Catal. 86 (1984) 400.
[26] R. Prins, V.H.J. de Beer, G.A. Somorjai, Catal. Rev.-Sci. Eng. 31 (1989) 1.
[27] H. Topsøe, B.S. Clausen, F.E. Massoth, Catal.: Sci. Technol. (1996).
[28] R.R. Chianelli, M. Daage, M.J. Ledoux, Adv. Catal. 40 (1994) 177.
[29] P. Raybaud, J. Hafner, G. Kresse, S. Kasztelan, H. Toulhoat, J. Catal. 190 (2000) 128.
[30] L.S. Byskov, J.K. Nørskov, B.S. Clausen, H. Topsøe, J. Catal. 187 (1999) 109.
[31] P. Raybaud, J. Hafner, G. Kresse, S. Kasztelan, H. Toulhoat, J. Catal. 189 (2000) 129.
[32] R.L. Wilson, C. Kemball, J. Catal. 3 (1964) 426.
[33] P. Kieran, C. Kemball, J. Catal. 4 (1965) 380.
[34] T. Todorova, Th. Weber, R. Prins, in press.
[35] H. Schulz, M. Schon, N.M. Rahman, Stud. Surf. Sci. Catal. 27 (1986) 201.
[36] M.D. Curtis, S.H. Druker, J. Am. Chem. Soc. 119 (1997) 1027.
[37] P. Kukula, A. Dutly, N. Sivasankar, R. Prins, J. Catal. 236 (2005) 14.
[38] A. Travert, H. Nakamura, R.A. van Santen, S. Cristol, J.F. Paul, E. Payen, J. Am. Chem. Soc. 124 (2002) 7084.
[39] J.V. Lauritsen, M.V. Bollinger, E. Lægsgaard, K.W. Jacobsen, J.K. Nørskov, B.S. Clausen, H. Topsøe, F. Besenbacher, J. Catal. 221 (2004) 510.